Atom Indonesia

Journal homepage: http://atomindonesia.brin.go.id

Atmospheric Plasma-Assisted Preparation of Graphene Oxide from Biomass: Characterization and Elemental Analysis

A. H. Handayani[1,2*], F. Amalia[2], E.V. Noviantana[3], T.R. Mulyaningsih[2], A. Waris[1], A. Dimyati[4]

[1]*Master Program in Nuclear Science and Engineering, Bandung Institute of Technology, Bandung, Indonesia*
[2]*Research Center for Nuclear Beam Analysis Technology, National Research and Innovation Agency, KST BJ Habibie, Serpong, Indonesia*
[3]*Directorate of Nuclear Power Facility Management, National Research and Innovation Agency, KST BJ Habibie, Serpong, Indonesia*
[4]*Directorate of Laboratory Management, Research Facilities, and Science and Technology Park, National Research and Innovation Agency, KST Soekarno, Cibinong, Indonesia*

ARTICLE INFO

Article history:
Received 6 May 2024
Received in revised form 25 November 2024
Accepted 3 December 2024

Keywords:

Graphene oxide
Atmospheric plasma
NAA
SEM-EDS
Biomass
Elemental analysis

ABSTRACT

Graphene oxide (GO) was successfully synthesized using the atmospheric plasma process with biomass precursors, including coconut fronds, palm fronds, and rambutan stems, within a five-minute processing time. Plasma technology converts near-waste materials into valuable resources with potential for various applications. Graphene oxide, in particular, exhibits high mechanical strength, excellent electrical conductivity, good biocompatibility, and a large surface area, making it a highly versatile material. Raman spectroscopy was used to analyze the formation of synthesized graphene. The presence of organic and inorganic elements in graphene oxide was characterized using a scanning electron microscope equipped with energy-dispersive X-ray spectroscopy (SEM-EDS) and neutron activation analysis (NAA). SEM-EDS analysis revealed that the C:O ratio in plasma-derived graphene oxide exceeded 80 % in each sample. NAA identified 22 inorganic elements, which are naturally present in biomass. Understanding the elemental composition of plasma-synthesized graphene oxide is essential for evaluating its potential applications and identifying necessary purification steps. The oxygen content in the synthesized material, which primarily originates from the inherent properties of biomass, can be regulated by optimizing plasma parameters. Using biomass precursors makes plasma-synthesized graphene oxide an economically viable option for large-scale production.

INTRODUCTION

Graphene is a two-dimensional (2D) carbon material known for its exceptional mechanical, optical, electrical, and thermal properties [1]. It can be synthesized using either bottom-up or top-down techniques [2]. The top-down approach typically involves exfoliating bulk materials into small pieces or sheets through mechanical, chemical, electrochemical, or thermal processes. Conversely, the bottom-up approach involves synthesizing graphene by combining molecules into graphene sheets or few-layer graphene using chemical, thermal, and catalytic techniques, such as SiC decomposition and chemical vapor deposition (CVD). However, the bottom-up approaches are generally complex and expensive [3]. Recent studies have introduced a bottom-up technique known as flash joule heating (FJH), which utilizes diverse carbon sources, such as coal, petroleum coke, biochar, carbon black, food waste, rubber tires, and mixed plastic waste, to produce high-quality graphene. This method achieves synthesis temperatures of approximately 3000 K, allowing rapid and efficient graphene production [4].

Graphene oxide (GO) is an oxygen-containing graphene derivative, with the edges of each layer terminated by carboxyl and carbonyl groups [3]. The most commonly used top-down method for synthesizing GO is the Hummers method, which uses graphite as a precursor. In this approach, graphite is oxidized to graphite oxide, followed by its exfoliation

*Corresponding author.
E-mail address: airine.hijrah.handayani@brin.go.id
DOI: https://doi.org/10.55981/aij.2025.1472

into GO [2,4]. Although effective, this method is time-consuming, requiring several hours to days [5,6]. Atmospheric plasma technology offers an alternative approach, capable of reaching temperatures as high as 3000 °C. In its application, plasma treatment has been used to convert oil palm fronds into reduced graphite oxide [7,8]. This technology enables the production of graphene and its derivatives with adjustable parameters, such as current (can be set from 8-100 ampere) and exposure time, which affect the resulting temperature and product characteristics. Additionally, the large plasma chamber can accommodate various plant biomass components, including stems, leaves, fruit peels, palm shells, and more.

Graphene and its derivatives have a wide range of applications, including biomedical, dentistry, material manufacturing, energy storage, optoelectronics, and nuclear technology [9–16]. In nuclear technology, GO has been explored for its application in removing radioactive contaminants, including uranium, and in synthesizing uranium carbide-graphene nanocomposites [11,12]. Additionally, GO holds promise as a separation membrane for the treatment of high-level liquid waste [17].

The elemental composition of plasma-treated samples is crucial for determining their potential applications and guiding further processing steps. The presence of organic elements, particularly carbon and oxygen, in plasma products can influence their optical properties and usability. For instance, oxygen-containing groups in graphene enhance its ability to absorb specific wavelengths in the infrared region and emit visible light [18]. Conversely, applications such as synthesizing uranium carbide-graphene nanocomposites require pure graphene without oxygen [12]. Inorganic elements in plasma products also contribute to functionality; for example, iron (Fe) in graphene oxide supports applications like water purification and pollutant degradation [19,20]. The oxygen content in plasma products, derived from the biomass precursor, can be controlled by adjusting plasma processing parameters.

Neutron activation analysis (NAA) is a sensitive, non-destructive analytical technique used for the qualitative and quantitative analysis of major, minor, trace, and rare elements [21-23]. This research focuses on identifying the elemental composition of plasma-treated products subjected to specific exposure times on various biomass materials, including coconut fronds, palm fronds, and rambutan stems. NAA and SEM-EDS were used to evaluate their potential applications or the need for further purification, while Raman spectroscopy confirms the formation of graphene.

METHODOLOGY

Material preparation

Biomass materials, including coconut fronds, palm fronds, and rambutan stems, were size-reduced and sun-dried for 3 hours. Each material, with dimensions of 28 mm long and 2 mm wide, was alternately arranged in a heat-resistant container and placed in the plasma chamber at a distance of 1 cm from the plasma torch. The plasma treatment was conducted for 5 minutes using a current of 80 amperes and argon gas at a flow rate of 10 liters per minute. Following the plasma process, the material was left in the plasma chamber for an additional 3 minutes under a continuous supply of argon gas to stabilize it. Plasma-treated samples were measured for electrical resistance and their electrical conductivity was calculated using Eq. (1). Samples with low resistivity, indicating high electrical conductivity, were then smoothed for further characterization of their organic and inorganic elemental composition. The plasma-treated samples were designated as coconut GO, palm GO, and rambutan GO. The preparation process is illustrated in Fig. 1.

$$\sigma = \frac{1}{\rho} \; ; \; \rho = R\frac{A}{l} \tag{1}$$

where:
σ = electrical conductivity (S/m)
ρ = resistivity (Ω m)
R = electrical resistance (Ω)
A = area of the sample (m^2)
l = length of the sample (m)

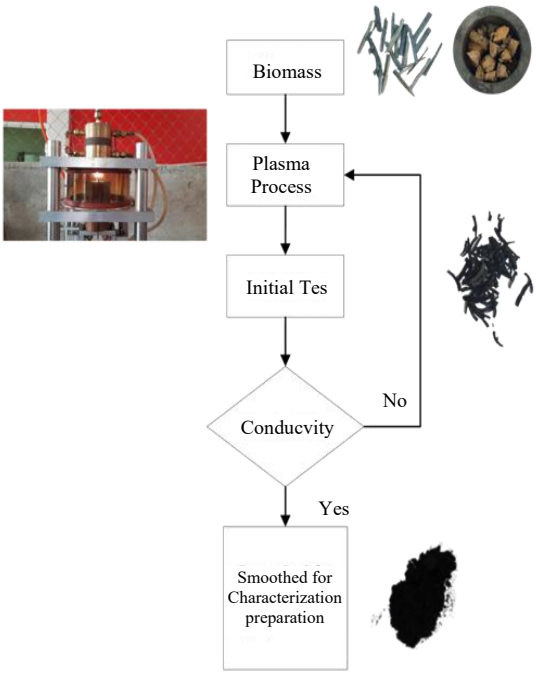

Fig. 1. Scheme of material preparation.

Material characterization

The samples were characterized using various techniques. Raman spectroscopy (Horiba Scientific) was employed to analyze the quality of graphene formation within the Raman shift range 0 – 3000 cm^{-1}. Raman spectroscopy examines the interaction of light with chemical bonds in molecules. When high-intensity light strikes a molecule, it scatters in various directions. Raman scattering occurs when light is scattered at different wavelengths, producing a spectrum with peaks that indicate the intensity and wavelength positions of the scattered light [24].

Graphene oxide powder samples were placed on double carbon tape attached to the sample holder. The samples were then analyzed for morphology and elemental composition using a scanning electron microscope with energy-dispersive X-ray (SEM-EDS). Organic elements, such as carbon and oxygen in powdered plasma GO, were analyzed using the SEM-EDS JEOL JSM-6510, which also detects inorganic elements.

Finally, the inorganic elements of powdered plasma GO were analyzed using neutron activation analysis (NAA). NAA qualitatively and quantitatively analyzes unknown samples by irradiating them with neutrons (n,γ) reactions and detecting the gamma (γ) rays emitted from radioactive nuclides post-irradiation. The gamma spectrum lines detected and recorded by the HPGe detector and its electronic circuit provide qualitative results [25]. Each polyethylene capsule was separately filled with 15 mg of powdered samples and standard reference materials. The activation (irradiation) of the samples and standard reference materials was performed under a thermal neutron flux $3.7x10^{13}\ n/cm^2\ dt^2$ in the research reactor rabbit system of G. A. Siwabessy. The elemental composition of plasma GO samples was quantified by comparing them with Peach Leaves NIST 1547 Standard Reference Material (SRM). The gamma-ray spectrometer included an HPGe detector with an electronic circuit, connected to a preamplifier, amplifier, ADC converter, and MCA. The measurements were conducted and analyzed using GENIE 2000 software from Canberra.

RESULTS AND DISCUSSION

Graphene oxide synthesis can be achieved using either top-down or bottom-up techniques. Top-down techniques involve converting graphite into graphene, whereas bottom-up approaches break down carbon-containing precursors [26]. The most commonly employed method is the Hummers method, which uses graphite as a carbon precursor [5,27–29]. However, this method demands substantial chemical usage and is time-consuming. Atmospheric plasma technology provides a rapid and efficient alternative for synthesizing GO, even when using near-waste biomass as a carbon precursor. Plasma treatment induces a graphitization process in the biomass, converting its cellulose, hemicellulose, and lignin structure into graphite under high temperatures [30]. Electrical conductivity, a key characteristic of graphite and graphene, can serve as an initial indicator of carbon-to-graphite transformation. The electrical conductivity values for the samples were approximately 930 S/m for coconut GO, 924 S/m for palm GO, and 936 S/m for rambutan GO, with the formulation obtained from the calculation using Eq. (1).

In addition to its electrical conductivity value, the quality of plasma-assisted GO was confirmed by Raman spectroscopy characterization and analysis of carbon content via SEM-EDS. Figure 2 illustrates the qualitative analysis of the graphitic samples, performed using Raman spectroscopy. The I_D/I_G ratio is an important parameter that provides information on the degree of disorder in graphene. The Raman spectra revealed the D and G bands characteristic of carbon nanostructures. The G-peak (graphite peak) corresponds to the bond stretching of sp^2 atoms in both rings and chains, while the D-peak arises from the breathing modes of sp^2 atoms in rings, commonly referred to as graphite defects [31–33]. Figure 2 highlights the defect peaks (D-band) for coconut GO, palm GO, and rambutan GO at Raman shift 1346 cm^{-1}, 1347 cm^{-1}, and 1371 cm^{-1} respectively, and the graphitic peak (G-band) at Raman shift 1571 cm^{-1}, 1585 cm^{-1}, and 1585 cm^{-1} respectively.

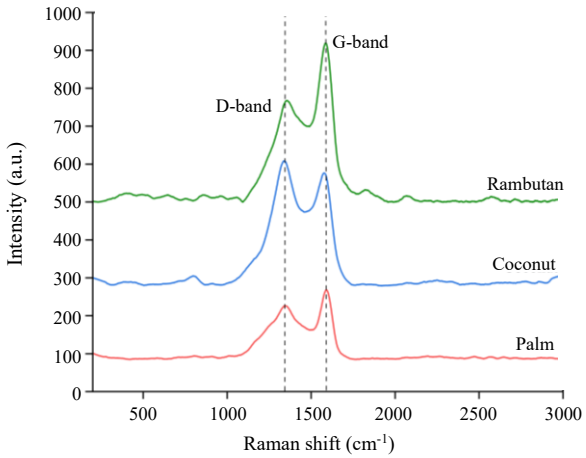

Fig. 2. Raman spectra of coconut, palm, and rambutan graphene oxide (GO).

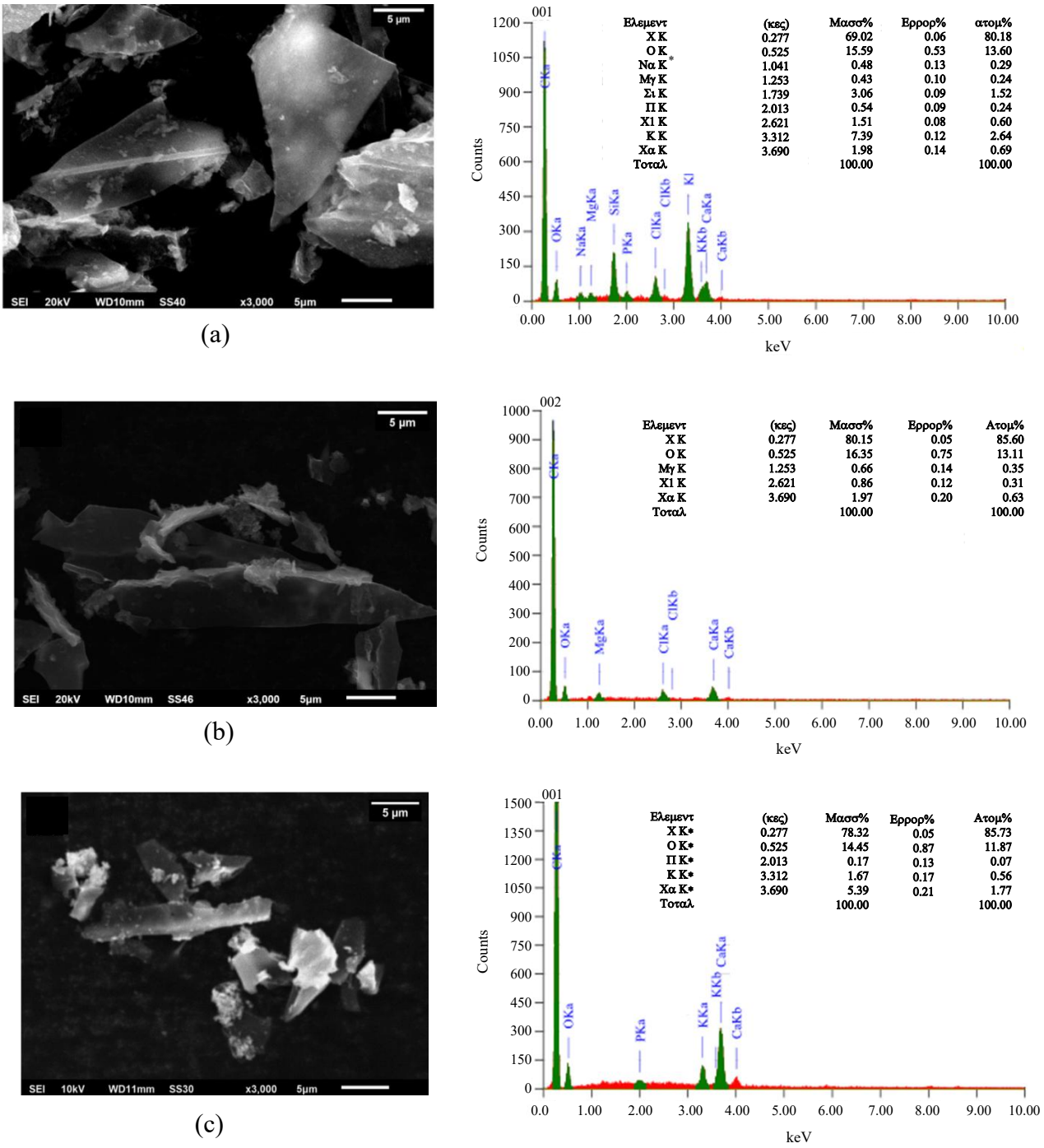

Fig. 3. SEM images corresponding EDS spectra of the (a) palm fronds, (b) coconut fronds, and (c) rambutan *stems* after the plasma process.

The intensity ratio (I_D/I_G) indicates the defect of the material. Low I_D/I_G indicates fewer defects, while a higher I_D/I_G ratio due to oxidation, introduces more defects [34]. In this research, the I_D/I_G ratios for coconut GO, palm GO, and rambutan GO were 1.16, 0.95, and 0.74, respectively. This implies that rambutan stems possess a more graphitic nature than palm and coconut fronds [35]. The I_D/I_G ratios are higher than graphite, signifying the presence of a graphene layer containing oxygen [36].

Plants typically require approximately 14 essential mineral elements for optimal growth and development [37]. For instance, rambutan plants contain minerals such as calcium (Ca), chromium (Cr), copper (Cu), iron (Fe), potassium (K), magnesium (Mg), manganese (Mn), sodium (Na), nickel (Ni), and zinc (Zn) [38,39]. Similarly, palm trees are reported to contain elements like iron (Fe), copper (Cu), zinc (Zn), cadmium (Cd), and arsenic (As) [40]. In coconut, a wide range of elements has been identified, including magnesium (Mg), calcium

(Ca), phosphorus (P), iodine (I), iron (Fe), selenium (Se), sodium (Na), zinc (Zn), chromium (Cr), aluminum (Al), antimony (Sb), arsenic (As), barium (Ba), boron (B), cobalt (Co), cesium (Cs), mercury (Hg), europium (Eu), nickel (Ni), rubidium (Rb), strontium (Sr), vanadium (V), molybdenum (Mo), tungsten (W), and cadmium (Cd) [41]. The elemental composition of plasma-assisted GO was analyzed using EDS and NAA.

The morphology of graphene oxide synthesized from biomass after plasma treatment is shown in Fig. 3, which confirms the formation of thin graphene sheets. The elemental composition, including organic and inorganic elements, was analyzed using EDS. Figure 3 provides detailed elemental composition data for the samples. Although several elements were present in the synthesized materials, their atomic ratios relative to carbon were minimal. This is attributed to the natural origin of the carbon source, which inherently includes essential plant nutrients. The carbon-to-oxygen (C:O) ratio is critical to GO formation. This ratio indicates the presence of GO, which typically contains a carbon-to-oxygen ratio of 3:1 [42]. On the atomic scale, the carbon content in palm GO, coconut GO, and rambutan GO was 80.18 %, 85.60 %, and 85.73 %, respectively, while the oxygen content was 13.60 %, 13.11 %, and 11.87 %, respectively. These results indicate that the C:O ratios in the three plasma-assisted samples exceed 3:1, verifying the presence of GO. Aside from carbon and oxygen, other trace elements present in very small atomic fractions included sodium (Na), magnesium (Mg), silicon (Si), phosphorus (P), chlorine (Cl), potassium (K), and calcium (Ca).

Neutron activation analysis (NAA) was employed as the preferred method for the elemental analysis of plasma-treated biomass samples due to its high sensitivity. The elemental concentrations were quantitatively determined by comparing the results with the Peach Leaves NIST 1547 standard reference material. A summary of the nuclear data for the elements identified in the plasma-treated biomass sample is presented in Table 1. The average elemental concentrations in the plasma biomass sample, as determined by NAA, are provided in Table 2.

Table 1. Nuclear data of the elements determined in plasma biomass.

Element	Activation Product	Energy Ex (keV)	Halflife
Na	^{24}Na	1368.6	14.96 h
K	^{42}K	1524.48	12.36 h
Ca	^{47}Ca	1297.09	4.54 d
Sc	^{46}Sc	889.28	83.81 d
Cr	^{51}Cr	320.08	27.7 d
Fe	^{59}Fe	1099.25	44.5 d
Co	^{60}Co	1173.24	5.27 y
Zn	^{65}Zn	1115.55	243.9 d
Br	^{82}Br	776.52	35.3h
Rb	^{86}Rb	1076.6	18.66 d
Sr	^{85}Sr	514	64.84 d
Sb	^{122}Sb	564.24	2.70 d
Cs	^{134}Cs	795.85	2.06 y
Ba	^{133}Ba	356.02	10.52y
La	^{140}La	1596.21	0.27 h
Ce	^{141}Ce	145.44	32.5 d
Eu	^{152}Eu	1408	13.33 y
W	^{187}W	479.57	23.9 h
Mg	^{27}Mg	1014.43	9.46 m
Mn	^{56}Mn	1810.72	2.58 h
Cl	^{38}Cl	1642.69	37.24 m
Al	^{28}Al	1778.99	2.24 m

Table 2. The average concentration of plasma biomass in µg/g determined by NAA.

Element	Palm GO			Coconut GO			Rambutan GO		
	Average	Acc. (%)	Detection Limits	Average	Acc. (%)	Detection Limits	Average	Acc. (%)	Detection Limits
Na	483.4±47.8	9.89	18.73	20930±314	1.50	39.52	74.99±2.92	3.90	17.16
K	59743±2469	4.13	2723	18087±1506	8.33	4422	5498±495	9.01	2597
Ca	39210±2078	5.30	1956	40430±1658	4.10	746.3	58840±2883	4.90	670.5
Sc	0.021±0.002	8.20	0.006	0.017±0.001	6.80	0.004	0.006±0.001	19.80	0.003
Cr	37.15±0.74	2.00	0.79	45.57±0.82	1.80	0.55	15.78±0.35	2.20	0.46
Fe	583.9±26.3	4.5	56.53	339.7±15.6	4.6	40.67	81.1±9.1	11.2	34.33
Co	1.23±0.05	4.10	0.10	2.24±0.71	31.60	0.07	4.65±0.54	11.70	4.42
Zn	87.82±2.46	2.80	3.33	28.00±1.29	4.60	2.50	38.14±2.02	5.30	2.12
Br	3.66±0.34	9.25	1.20	22.77±1.40	6.13	4.97	1.04±0.09	8.60	1.12
Rb	203.4±4.3	2.10	2.81	70.8±1.8	2.60	1.94	58.1±2.2	3.80	1.61
Sr	214.9±12.3	5.70	33.15	300.5±15.9	5.30	25.16	168.0±13.3	7.90	21.23
Sb	0.52±0.03	5.50	0.08	0.12±0.02	20.00	0.06	0.11±0.02	19.80	0.05
Cs	1.46±0.05	3.60	0.07	7.44±0.15	2.00	0.05	6.59±0.16	2.40	0.05
Ba	0	0	0	73.68±3.91	5.30	11.11	30.32±4.49	14.80	9.49
La	0.64±0.08	13.20	0.47	1.73±0.35	20.00	0.89	2.04±0.07	3.60	0.47
Ce	115.0±2.0	1.70	0.70	3.1±0.6	17.60	0.33	36.1±0.9	2.40	0.31
Eu	0	0	0	0.042±0.005	11.50	0.01	0.091±0.005	5.70	0.01
W	11.19±0.65	5.80	1.85	21.49±1.68	7.80	3.88	439.3±6.6	1.50	1.96
Mg	12613±730	5.79	729.8	10891±869	7.98	869.2	2916±612	20.99	612.0
Mn	77.30±2.05	2.65	2.05	236.3±4.3	1.82	4.31	1551±37	2.40	37.15
Cl	5637±233	4.12	232.5	22439±1246	5.55	1246	420±39	9.27	38.97
Al	348.2±27.0	7.74	26.95	0	0	0	218.9±26.0	11.87	25.99

From the analysis, 22 elements were identified in the plasma-assisted GO samples. Short-lived isotopes such as ^{47}Ca, ^{27}Mg, ^{56}Mn, ^{38}Cl, and ^{28}Al were detected when the samples were activated for a short duration of 60 seconds. The elemental ratio distribution of short-lived isotopes is shown in Fig. 4. Medium-lived isotopes, including ^{24}Na, ^{42}K, ^{82}Br, ^{122}Sb, ^{133}Ba, and ^{187}W were identified when the samples were activated for 30 minutes. The elemental ratio distribution of these medium-lived isotopes is illustrated in Fig. 5. Long-lived isotopes such as ^{46}Sc, ^{51}Cr, ^{59}Fe, ^{60}Co, ^{65}Zn, ^{86}Rb, ^{85}Sr, ^{134}Cs, and ^{152}Eu were detected when the samples were activated for 3 hours. The elemental ratio distribution of these long-lived isotopes is presented in Fig. 6.

Furthermore, the concentration of two rare earth elements (REE), lanthanum (La) and cerium (Ce), were quantified in plasma GO samples. The measurement accuracy for La and Ce was determined at 13.2 % and 1.7 % in the palm sample, 20.0 % and 17.6 % in the coconut sample, and 3.6 % and 2.4 % in the rambutan sample, respectively.

Table 3. Internal quality control of eements measurement using Neutron Activation Analysis (NAA) method across Peach Leaves Standard Reference Materials.

Elements	Concentration in µg/g		
	Current study	Certificate	Ratio**
Ba	115.8 ± 8.5	123.7 ± 5.5	0.94
Br	12.8 ± 2.5	11*	1.16
Ca	14920 ± 240	15590 ± 160	0.96
Ce	10.36 ± 1.46	10.00*	1.04
Co	0.067 ± 0.01	0.07*	0.96
Eu	0.18 ± 0.01	0.17*	1.05
Fe	250.5 ± 10.4	219.8 ± 6.8	1.14
K	24650 ± 567	24330 ± 380	1.01
La	10.23 ±1.01	9.00*	1.14
Rb	21.95 ±1.25	19.65 ± 0.89	1.12
Sc	0.04 ± 0.01	0.04*	1.00
Sr	58.58 ± 5.41	53.0 ± 5.0	1.10
Zn	20.61 ± 1.12	17.97 ± 0.53	1.15
Mg	4428 ± 299	4320 ± 150	1.03
Mn	96.10 ± 4.44	97.8 ± 1.8	0.98
Cl	421.74 ± 26.93	361 ± 14	1.16

Note: * Non-certified value, ** Ratio the experimental result to certificate value

Internal quality control was conducted by analyzing the standard reference material (SRM) 1547 Peach Leaves alongside the research samples to validate the NAA method employed. The quality control results are summarized in Table 3. The elemental analysis outcomes were compared to the certified values, and the R-value (the ratio of analysis results to SRM-certified values) was calculated. The R-values ranged from 0.94 to 1.16, demonstrating close agreement with the certified values and confirming the validity of the analytical method. In the palm GO sample, barium (Ba), and europium (Eu) concentrations were below the detection limits of 0.124 µg/g and 0.151 µg/g, respectively, and therefore could not be detected. Additionally, the aluminium (Al) concentration in coconut GO could not be reported due to the prolonged decay time between irradiation and measurement. The isotope decayed completely before detection given the short half-life of ^{28}Al (134.4 seconds).

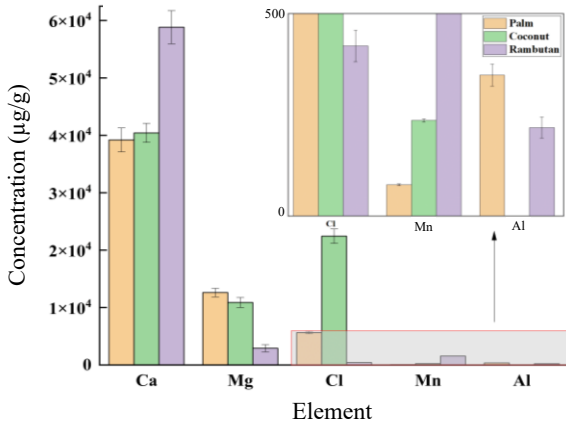

Fig. 4. The elemental ratio distribution of short-lived isotopes.

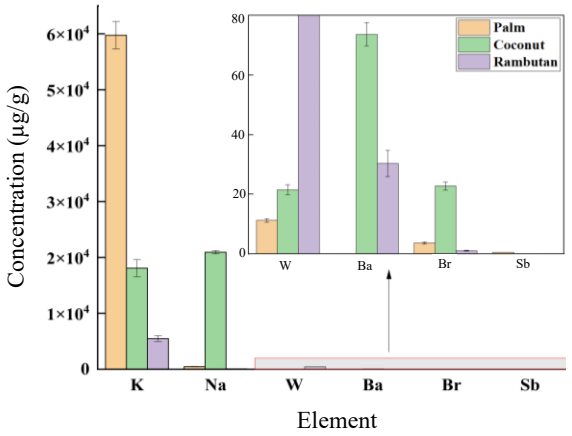

Fig. 5. The elemental ratio distribution of medium-lived isotopes.

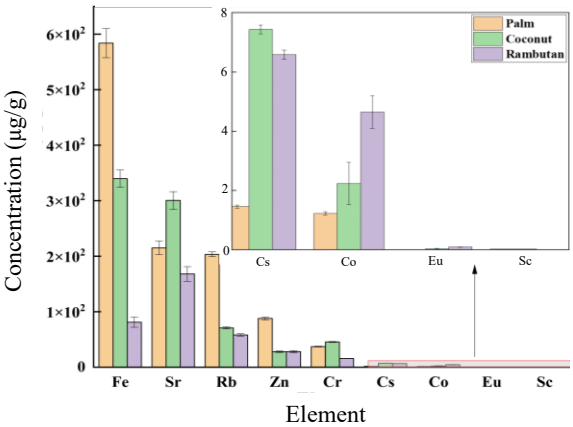

Fig. 6. The elemental ratio distribution of long-lived isotope.

Macro and microelements in plant-derived samples cannot be eliminated with only 5 minutes of plasma treatment, as these elements are present in trace amounts (μg/g scale) compared to the primary elements, carbon (C) and oxygen (O). This elemental retention should be considered for the potential applications of plasma-assisted GO. For instance, the plasma-generated GO synthesized in this study, containing iron (Fe) as a dopant element, may be suitable for water purification and pollutant degradation applications. Conversely, if pure graphene without trace elements is required, alternative plasma treatments must be explored. These may include extending plasma exposure time, increasing plasma current and argon gas flow rate, and implementing additional purification steps, such as washing with distilled water or acidic solutions, to effectively remove residual heavy metals from plant-based precursors [8,43].

CONCLUSION

Graphene oxide was successfully synthesized from biomass precursors using atmospheric plasma exposure for 5 minutes. Raman spectroscopy confirmed the formation of GO, with the calculated intensity ratios of D-peak and G-peak as follows: coconut GO, (1.16), palm GO, (0.95), and rambutan GO (0.74). Energy-dispersive spectroscopy (EDS) via SEM revealed a carbon-to-oxygen (C:O) ratio exceeding 80 % in all samples. Neutron activation analysis (NAA) identified 22 elements, including Na, K, Ca, Sc, Cr, Fe, Co, Zn, Br, Rb, Sr, Sb, Cs, Ba, La, Ce, Eu, W, Mg, Mn, Cl, and Al. Understanding the elemental composition of the plasma-derived product is essential, particularly for applications or further purification processes that may be required. Moreover, atmospheric plasma technology shows significant potential for converting near-waste materials into high-value resources. Its rapid synthesis process and scalability make it a promising approach for large-scale production.

ACKNOWLEDGMENT

The authors express their gratitude to the Research Organization for Nuclear Energy and the Research Organization for Nanotechnology and Materials for providing material support for this research. Acknowledgment is also extended to the Neutron Scattering Laboratory and the G.A. Siwabessy Research Nuclear Reactor, National Research and Innovation Agency, for the facilities and scientific and technical support accessed through E-Layanan Sains, National Research and Innovation Agency. Special thanks are directed to the Head of the Research Center for Nuclear Beam Analysis Technology for his invaluable assistance in the execution of this research.

AUTHOR CONTRIBUTION

A. H. Handayani is the main contributor. A. Dimyati and A. Waris contributed to the conceptualization and provided additional support. F. Amalia, E. V. Noviantana, and T. R. Mulyaningsih are supporting contributors to this paper. All authors have read and approved the final version of the paper.

REFERENCES

1. R. Rudrapati, *Graphene: Fabrication Methods, Properties, and Applications in Modern Industries*, in: Graphene Production and Application, IntechOpen, UK (2020) 1.
2. A. Gutiérrez-Cruz, A. R. Ruiz-Hernández, J. F. Vega-Clemente et al., J. Mater. Sci. **57** (2022) 14543.
3. A. Ambrosi, C. K. Chua, A. Bonanni *et al.,* Chem. Rev. **114** (2014) 7150.
4. D. X. Luong, K. V. Bets, W. A. Algozeeb *et al.,* Nature **577** (2020) 647.
5. H. Yu, B. Zhang, C. Bulin *et al.*, Sci. Rep. **6** (2016) 36143.
6. N. Ciptasari, N. Darsono, M. Handayani *et al.*, *Synthesis of graphite oxide using hummers method: Oxidation time influence*, in: Proceedings of the 4th International Seminar on Metallurgy and Materials (ISMM2020) (2021) 020010.
7. A. H. Handayani, E. V. Noviantana, Bharoto *et al.*, *Development of a Small Central Control Unit for the Automated Universal Arc Plasma Sintering (U-APS) using Raspberry Pi 3B+ Microcomputer,* in: Proceeding International Conference on Nuclear Science, Technology, and Application (2021) 271.
8. R. I. Purawiardi, A. Dimyati, A. H. Handayani *et al., Plasma-Assisted Pyrolysis for Converting Oil Palm Fronds Into Reduced Graphite Oxide,* in: IOP Conference Series: Earth and Environmental Science (2024).
9. T. M. Magne, T. D. O. Vieira, L. M. R. Alencar *et al.*, J. Nanostructure Chem. **12** (2021) 693.

10. J. Pei, T. Ren, Y. Huang *et al.,* Front. Chem. **10** (2022) 1.
11. S. Verma and K. H. Kim, Environ. Int. **158** (2022) 106944.
12. L. Biasetto, S. Corradetti, S. Carturan *et al*., Sci. Rep. **8** (2018) 8272.
13. A. Cai, R. E. Horch, J. P. Beier, *Nanofiber Composites in Skeletal Muscle Tissue Engineering,* in: Nanofiber Composites for Biomedical Applications, Elsevier Inc., Cambridge (2017) 369.
14. X. Wang, S. Yu, J. Jin *et al.,* Sci. Bull. **61** (2016) 1583.
15. N. Pan, D. Guan, T. He et al., J. Radioanal. Nucl. Chem. **298** (2013) 1999.
16. J. H. Kim, S. Kim, S. Song *et al*., Photonics **8** (2021) 543.
17. H. Zhao, J. Yang, Z. Li, J. Clean Prod. **266** (2020) 121884.
18. H. R. Thomas, C. Vallés, R. J. Young *et al.,* J. Mater. Chem. C. 1 (2013) 338.
19. A. K. Tolkou, A. I. Zouboulis, C (Journal of Carbon Research) **6** (2020) 44.
20. G. H. Le, T. T. Nguyen, M. B. Nguyen *et al.,* Top. Catal. **63** (2020) 1314.
21. A. Kirillov, D. Grozdov, I. Zinicovscaia *et al.*, J. Radioanal. Nucl. Chem. **331** (2022) 249.
22. R. R. Greenberg, P. Bode and E. A. D. N. Fernandes, Spectrochim. Acta Part B: At. Spectrosc. **66** (2011) 193.
23. N. Salim, M. Santoso, S. Damayanti *et al*., Atom Indones. **38** (2013) 13.
24. S. Eigler, and A. M. Dimiev, *Characterization Techniques*, in: Graphene Oxide: Fundamentals and Applications, John Wiley & Sons, Inc. West Sussex (2017) 87.
25. A. El-Taher and M. A. K. Abdelhalim, J. Radioanal. Nucl. Chem. **299** (2014) 1949.
26. A. Adetayo and D. Runsewe, Open Journal of Composite Materials **09** (2019) 207.
27. R. Muzyka, M. Kwoka, Ł. Smędowski *et al.*, New Carbon Mater. **32** (2017) 15.
28. A. Alkhouzaam, H. Qiblawey, M. Khraisheh *et al.,* Ceram. Int. **46** (2020) 23997.
29. D. C. Marcano, D. V. Kosynkin, J. M. Berlin, *et al.*, ACS Nano **4** (2010) 4333.
30. M. A. A. Farid and Y. Andou, J. Clean. Prod. **380** (2022) 135090.
31. A. C. Ferrari and J. Robertson, Phys. Rev. B **61** (2000) 14095.
32. V. Scardaci and G. Compagnini, C (Journal of Carbon Research) **7** (2021) 48.
33. J. Xu, Q. He, Z. Xiong *et al.*, Energy and Fuels **35** (2020) 2870.
34. M. S. Khan, R. Yadav, R. Vyas, *Synthesis and Evaluation of Reduced Graphene Oxide for Supercapacitor Application*, in: Mater Today Proceedings, Elsevier Ltd (2020) 153.
35. B. A. Widyaningrum, D. Apriani, P. Amanda *et al.,* Jurnal Sains Materi Indonesia **22** (2021) 101. (in Indonesian)
36. S.-G. Kim, O.-K. Park, J. H. Lee *et al.*, Carbon Lett. **14** (2013) 247.
37. R. Vatansever, I. I. Ozyigitand E. Filiz, Appl Biochem. Biotechnol. **181** (2017) 464.
38. S. Torgbo, P. Rugthaworn, U. Sukatta *et al*., ACS Omega **7 (**2022) 34647.
39. R. Bhat, *Bioactive Compounds of Rambutan (Nephelium lappaceum L.),* in: Bioactive Compounds in Underutilized Fruits and Nuts, Springer, Cham (2019) 1.
40. H. Thompson-Morrison, S. Gaw and B. Robinson, Sustainability **14** (2022) 4553.
41. Anonymous, Coconut Tree Characteristics. http://www.botanical-online.com/en/botany /coconut-tree, Retrieved in October (2023).
42. I. Tiginyanu, V. Ursaki, V. Popa, *Ultra-Thin Membranes for Sensor Applications,* in: Nanocoatings and Ultra-Thin Films, Elsevier, (2011) 330.
43. H. Song, J. Zhou, S. He, Int. J. Environ. Res. Public Health **20** (2023) 1311.